ON THE SPECTRUM OF LATTICE MASSIVE SU(2) YANG–MILLS

Ruggero Ferrari

INFN, Sezione di Milano, via Celoria 16, 20133 Milano, Italy
and
Center for Theoretical Physics
Laboratory for Nuclear Science and Department of Physics
Massachusetts Institute of Technology
Cambridge, Massachusetts 02139, USA
ruggero.ferrari@mi.infn.it

(Received July 4, 2013)

On the basis of extended simulations, we provide some results concerning the spectrum of Massive SU(2) Yang–Mills on the lattice. We study the "time" correlator of local gauge invariant operators integrated over the remaining three dimensions. The energy gaps are measured in the isospin $I = 0, 1$ and internal spin $J = 0, 1$ channels. No correlation is found in the $I = 1$, $J = 0$ channel. In the $I = 1$, $J = 1$ channel and far from the critical mass value m_c, the energy gap roughly follows the bare value m (vector mesons). In approaching the critical value m_c at β fixed, there is a bifurcation of the energy gap: one branch follows the value m, while the new is much larger and it shows a more and more dominant weight. This phenomenon might be the sign of two important features: the long range correlation near the fixed point at $\beta \to \infty$ implied by the low energy gap and the screening (or confining) mechanisms across the $m = m_c$ associated to the larger gap. The $I = 0$, $J = 0, 1$ gaps are of the same order of magnitude, typically larger than the $I = 1$, $J = 1$ gap (for $m \gg m_c$). For $m \sim m_c$, both $I = 0$ gaps have a dramatic drop with minima near the value m. This behavior might correspond to the formation of $I = 0$ bound states both in the $J = 0$ and $J = 1$ channels.

DOI:10.5506/APhysPolB.44.1871
PACS numbers: 11.15.Ha, 11.30.Rd, 12.60.Rc

1. Introduction

In the present paper, we continue the study of the Massive SU(2) Yang–Mills (MYM) theory on the lattice, initiated in Ref. [1] and further pursued in Ref. [2]. Let us remind why we consider the model to be of great interest. Recently, a Massive Yang–Mills theory for SU(2) has been formulated

in the continuum in Refs. [3, 4]. The mass is introduced *à la* Stückelberg. Since the theory is nonrenormalizable, a new subtraction strategy is necessary. The strategy has been developed in a series of papers [5–7] and it is based on a Local Functional Equation (LFE) for the vertex functional and on dimensional subtraction. Although the subtraction procedure has been successfully applied to massless [5] and massive [8] nonlinear sigma model, to the low energy electroweak model [9–11] and to field-coordinate transformations [12], still nonrenormalizability has unpleasant consequences for the high energy behavior in most of the listed cases (unitarity violations). It has been suggested that such nonrenormalizable theories, once made finite by the appropriate subtraction strategy, undergo to a phase transition [13, 14] at very large energies. This conjecture might be investigated in a nonperturbative approach, as in a lattice model. This is the rationale for considering a Massive Yang–Mills lattice gauge theory: the model has the same local gauge symmetry as in the continuum and one has the possibility to avoid completely any gauge fixing. The challenge consists in comparing the lattice and the continuum amplitudes, in mapping the parameters and in evaluating the limit of validity of the lattice model as a phenomenological theory. In [1], the existence of a Transition Line (TL) $m = m_{\rm TL}(\beta)$ in the (β, m^2) space has been confirmed. Along this line, from the end-point $\beta_{\rm e} \sim 2.2$ through $\beta \to \infty$, both energy and order parameter have a very steep inflection, whose derivative increases with the lattice size (as discussed later in Sec. 2). The line separates the deconfined phase from a supposedly confined phase. For $\beta < \beta_{\rm e}$, the transition through the line is smooth. Thus we denote the TL by $m = m_{\rm c}(\beta)$ for $\beta > \beta_{\rm e}$.

In Ref. [2], we have compared global quantities as energy and order parameter evaluated by Monte Carlo in the lattice and two-loop calculations in the continuum. The results are suggestive of a good agreement.

The present paper is devoted to the investigation of the particle content of the Massive Yang–Mills on the lattice in the deconfined region of the parameter space (β, m^2). We look at the energy gap in the time correlator of suitable gauge invariant operators mediated over the other dimensions (zero three-momentum states). These operators are easily associated to particles with isospin $I = 0, 1$ and spin $J = 0, 1$ in the deconfined phase. The fit is done with the function

$$\begin{aligned} g(x) &= \tfrac{1}{2}(f(x) + f(L-x))\,, \\ f(x) &= b_1 e^{-\Delta_1 x} + b_2 e^{-\Delta_2 x}\,, \end{aligned} \tag{1}$$

where L is the size of the lattice (an integer) and L^4 gives the number of the lattice sites. We considered mainly lattices of size 24^4 and the measures are performed on 10^4 configurations each separated by 15 updatings. Statistical errors are evaluated by using bins of size 100.

This excruciating analysis is limited to few values of $\beta = 1.5, 3, 10, 40$, being the end-point $\beta_e \sim 2.2$. We find no correlation in the channel $I = 1$, $J = 0$; *i.e.* no scalars with flavor 1. In the channel $I = 1$, $J = 1$ (gauge vector mesons) the value of the gap is close to the bare mass m for $m \geq 1$. For m near m_c (thus $\beta = 1.5$ excluded), a bifurcation occurs, *i.e.* the fit requires two energy gap parameters. The lower follows the m value while the second is much larger. *A posteriori* this bifurcation looks necessary if we expect a large correlation length near $\beta \to \infty$ ($\Longrightarrow m_c \to 0$) and a larger gap for the establishment of confinement across the TL.

A similar situation is present in the channels $I = 0$, $J = 0, 1$; however, the bifurcation sets on nearer the TL than in the vector mesons channel. The numerical values, in general, follow the pattern $\Delta_{I=0\,J=1} \simeq \Delta_{I=0\,J=0} \gg m$. For $m \sim m_c$, the lower energy gap in the $I = 0$ channels drops to values of the order of m. In this region, the larger gap in the $I = 1$, $J = 1$ channel is dominant; therefore, long living resonant states might develop in the $I = 0$, $J = 0, 1$ channels.

This scenario of the spectrum opens many interesting questions. We mention here a couple of them. The onset of confinement across the TL for $\beta \gg \beta_e$ is clearly related to the bifurcation of gap when $m \to m_c$. The present work spots the point where it is possible to study the mechanism of confinement at its onset. A further question of great interest is whether a bound state of two vector mesons exists near the TL, *i.e.* where the correlation length becomes larger. We shall illustrate this phenomenon with some pictures later on.

The lattice model is of great interest by itself: the phase diagram in the parameter space (β, m^2) is very intriguing. The TL at large β is compatible with $\beta m^2 \sim 0.64$, *i.e.* the TL points to the critical point of the $O(4)$ nonlinear sigma model [15].

The same lattice gauge model has been studied previously (see [16–23]) as an example of Higgs mechanism with a frozen length. We agree on the position of the TL, but we have no definite results on the exact nature of the phase transition, beyond the presence of a steep inflection which becomes more and more strong by increasing β.

Further work is necessary in order to establish the character of the phase transition across the TL. Moreover, it is very important to interpret the model in the limit of $\beta \to \infty$, where a fixed point is expected [24]. In the limit, some correlation length should become very large.

The relation between the lattice model and the continuum theory is not discussed here. We postpone this complex topic to a future work.

2. The model

The present section is devoted to the recollection of the essentials of the model. More details are given in Refs. [1] and [2].

The action on the cubic lattice of size $N \equiv L^4$ with sites x and links μ is

$$\begin{aligned} S_L \;=\; & \frac{\beta}{2}\,\mathfrak{Re}\sum_{\square}\mathrm{Tr}\{1-U_{\square}\} \\ & +\frac{\beta}{2}m^2\mathfrak{Re}\sum_{x\mu}\mathrm{Tr}\Big\{1-\Omega(x)^{\dagger}U(x,\mu)\Omega(x+\mu)\Big\}\,, \end{aligned} \tag{2}$$

where the sum over the plaquette is the Wilson action [25]. The link variables $U(x,\mu)$ and the site variables $\Omega(x)$ are elements of the SU(2) group.

The action is invariant under the **local-left** transformations $g_{\mathrm{L}}(x) \in \mathrm{SU}(2)_{\mathrm{L}}$ and the **global-right** transformations $g_{\mathrm{R}} \in \mathrm{SU}(2)_{\mathrm{R}}$

$$\begin{aligned} &\mathrm{SU}(2)_{\mathrm{L}}\begin{cases} \Omega'(x) = g_{\mathrm{L}}(x)\Omega(x) \\ U'(x,\mu) = g_{\mathrm{L}}(x)U(x,\mu)g_{\mathrm{L}}^{\dagger}(x+\mu) \end{cases}, \\ &\mathrm{SU}(2)_{\mathrm{R}}\begin{cases} \Omega'(x) = \Omega(x)g_{\mathrm{R}}^{\dagger} \\ U'(x,\mu) = U(x,\mu) \end{cases}. \end{aligned} \tag{3}$$

We would like to stress the importance of this invariance property, in particular because in the nonrenormalizable continuum Minkowskean theory it is the starting point for the removal of the ultraviolet divergences of the loop expansion. In fact, the invariance of the path integral measure ensures the validity of the LFE for the generating functionals (*e.g.* the vertex functional) [5].

The quantity ($D = 4$)

$$\mathfrak{C} := \frac{1}{2DN}\left\langle \sum_{x\mu}\mathrm{Tr}\Big\{\Omega(x)^{\dagger}U(x,\mu)\Omega(x+\mu)\Big\}\right\rangle \tag{4}$$

is taken as an order parameter. It has the symmetry property $\mathfrak{C}(\beta,-m^2) = \mathfrak{C}(\beta,m^2)$. The TL is given by the *loci* in the (β,m^2) plan, where $\mathfrak{C}$ has an inflection as function of m^2 for given β as shown in Fig. 1.

For large β, the TL approaches the critical coupling $\beta m^2 \sim 0.64$ of the SU(2) nonlinear sigma model in 4 dimensions [15]. Moreover, in the region $\mathfrak{C} \sim 0$, the global-right $\mathrm{SU}(2)_{\mathrm{R}}$ charges are screened (or confined), while for $\mathfrak{C} \sim \pm 1$ the global-right $\mathrm{SU}(2)_{\mathrm{R}}$ is unitarely implemented and vector mesons exist.

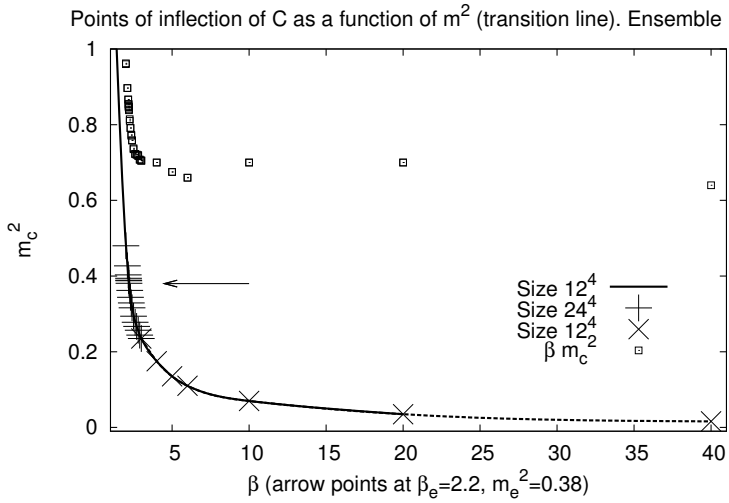

Fig. 1. The transition line. The arrow marks the position of the end-point. In the figure data from previous analysis have been used and the statistical errors are not displayed since they are too small to be shown.

The character of the transition across the TL is not yet well established. The inflection becomes steeper by increasing the lattice size for β larger than the end-point value: $\beta_{\rm e} \sim 2.2, m_{\rm e}^2 \sim 0.381$. Numerically, one cannot easily affirm whether it is a first order transition with a small jump or a second order or even a crossover. This question is not under investigation in the present paper.

3. Gauge invariant fields

In order to investigate the spectrum in the deconfined region in the (β, m^2) plan, we consider the field (τ_a are the Pauli matrices)

$$C(x,\mu) := \Omega^\dagger(x) U(x,\mu) \Omega(x+\mu) = C_0(x,\mu) + i\tau_a C_a(x,\mu)\,. \tag{5}$$

By construction,

$$C(x,\mu) \in \mathrm{SU}(2)\,. \tag{6}$$

According to the transformations of Eq. (3), $C(x,\mu)$ is invariant under local-left transformations (usually said "gauge invariant"), while under the global-right transformations they have $I = 0$ (C_0) and $I = 1$ components (C_a). One has

$$C_0(x,\mu)^2 + \sum_{a=1,3} C_a(x,\mu)^2 = 1\,. \tag{7}$$

Then, we get

$$|C_0(x,\mu)| \leq 1 \tag{8}$$

and, therefore, (from Eq. (4))

$$|\mathfrak{C}| \leq 1\,. \tag{9}$$

In the deconfined region, we expect the global-right symmetry to be implemented and, therefore,

$$\begin{aligned} &\langle C_a(x,\mu)\rangle = 0\,,\\ &\langle C_a(x,\mu)C_b(y,\nu)\rangle = 0\,, \quad \text{if} \quad a \neq b\,. \end{aligned} \tag{10}$$

Moreover, the symmetry over four-dimensional finite rotations requires

$$\langle C_a(x,\mu)C_a(y,\nu)\rangle = 0\,, \quad \text{if} \quad \mu \neq \nu\,. \tag{11}$$

Equations (9), (10) and (11) are satisfied by the numerical simulations to a reasonable level of accuracy.

4. The numerical simulation

The spectrum is evaluated in the deconfined phase, by considering the two-point function of the zero-three-momentum operator

$$C_j(t,\mu) = \frac{1}{L^{\frac{3}{2}}} \sum_{x_1,x_2,x_3} C_j(x_1,x_2,x_3,x_4,\mu)|_{x_4=t}\,, \qquad j = 0,1,2,3\,. \tag{12}$$

Then, we evaluate the connected correlator

$$C_{jj',\mu\nu}(t) = \frac{1}{L} \sum_{t_0=1,L} \Big\langle C_j(t+t_0,\mu)C_{j'}(t_0,\nu)\Big\rangle_C\,. \tag{13}$$

According to Eqs. (10) and (11), the correlator is zero unless $j = j'$ and $\mu = \nu$. The spin one- and zero-amplitudes V and S are extracted by using the relation

$$C_{jj,\mu\nu}(t) = V_{jj}\,(\delta_{\mu\nu} - \delta_{\mu 4}\delta_{\nu 4}) + S_{jj}\delta_{\mu 4}\delta_{\nu 4}\,. \tag{14}$$

A very good fit of the data is obtained by using the function

$$\begin{aligned} g(t) &= \tfrac{1}{2}(f(t) + f(L-x))\,,\\ f(t) &= b_1 e^{-\Delta_1 t} + b_2 e^{-\Delta_2 t}\,. \end{aligned} \tag{15}$$

Two exponentials are needed only for $m \simeq m_c$, as we will illustrate shortly. Otherwise, one single exponential is enough for the fit.

The expectation values are performed on 10^4 configurations created by a Heat-Bath Monte Carlo for a lattice of size 24^4. A configuration is stored every 15 updating steps. Statistical errors are evaluated by using bins of 100 measures. We consider the values $\beta = 1.5, 3, 10, 40$ and $m^2 < 8$. The first is interesting since it is outside the TL (the "end point" is at $\beta_e \sim 2.2$). For $\beta = 3$, the TL separates different phases and the "coupling constant" ($g = \sqrt{4/\beta} \sim 1.155$) is large, while for $\beta = 40$, we are in the region of weak coupling limit ($g \sim 0.316$) and "near" the fixed point $\beta \to \infty$.

Figures 2, 3, 4 and 5 illustrate the fact that for $m^2 \gg m^2_{\text{TL}}$ gauge vector mesons are present in the spectrum of the lattice Massive Yang–Mills theory (2). The mass (Δ_1) follows roughly the bare value m and looks not to depend much on β. The fit shown in the figures is performed by using the function

$$\sqrt{m^2}\,\left[1 + (A \ln m^2 + B)\right] \tag{16}$$

inspired by the expression of the self-energy in perturbation theory. It parameterizes the departure of the gap from the bare value m.

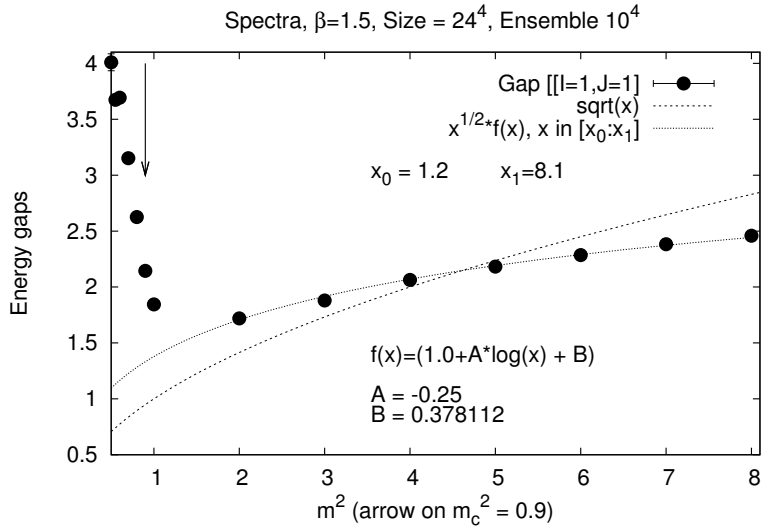

Fig. 2. Mass spectrum of the gauge vector meson for $\beta = 1.5$.

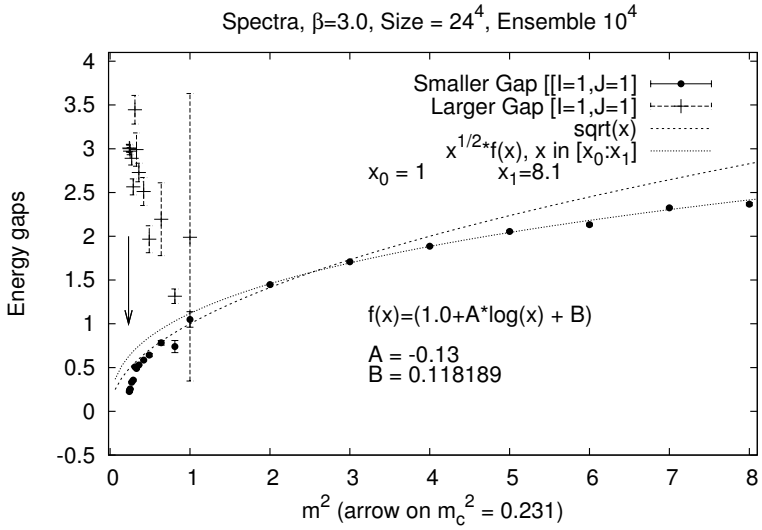

Fig. 3. Mass spectrum ($m \gg m_c$) of the gauge vector meson for $\beta = 3$.

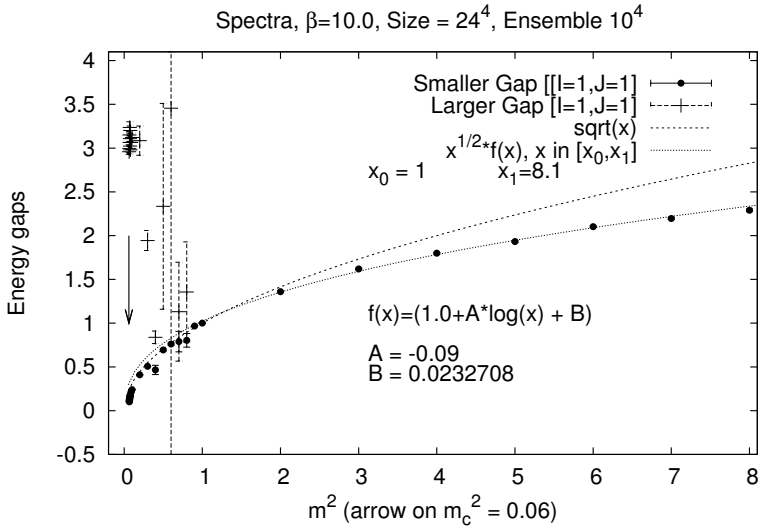

Fig. 4. Mass spectrum ($m \gg m_c$) of the gauge vector meson for $\beta = 10$.

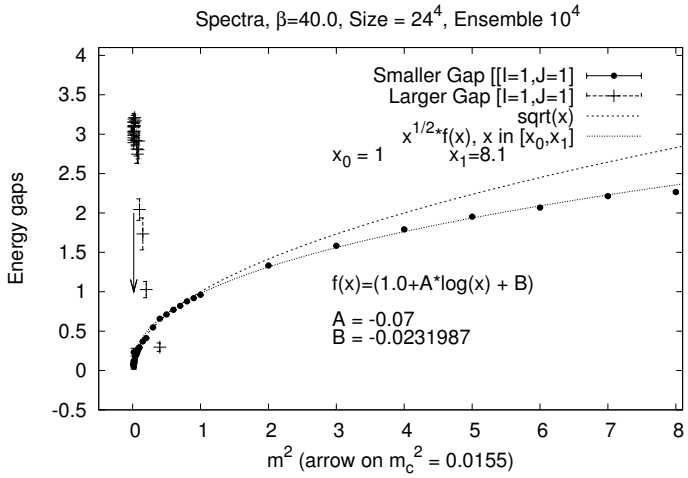

Fig. 5. Mass spectrum ($m \gg m_c$) of the gauge vector meson for $\beta = 40$.

The scalar isospin ($I = 0$) states have spin zero ($J = 0$) and spin ($J = 1$). Figures 6, 7, 8 and 9 show the numerical results. The patterns are not as clear as in the case of $I = 1$. The energy gaps are much larger than m. These states are not present in the naive continuum limit of zero spacing, if perturbation theory is used.

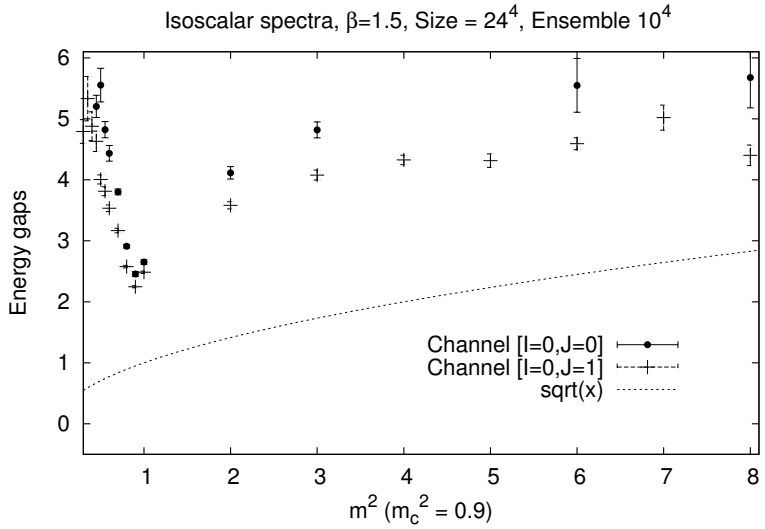

Fig. 6. Mass spectrum of the isoscalars for $\beta = 1.5$.

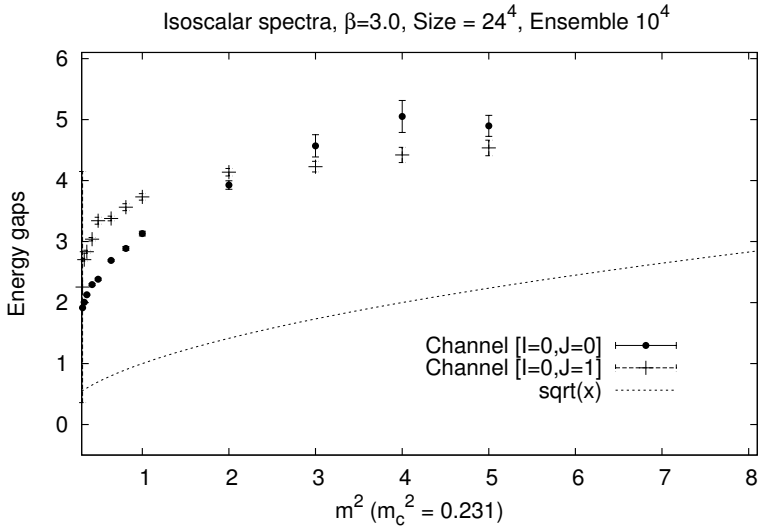

Fig. 7. Mass spectrum ($m \gg m_{\mathrm{c}}$) of the isoscalars for $\beta = 3$.

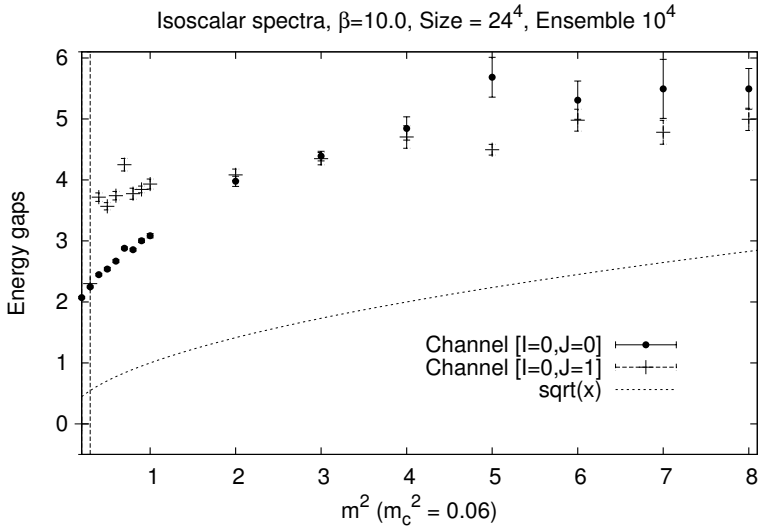

Fig. 8. Mass spectrum ($m \gg m_{\mathrm{c}}$) of the isoscalars for $\beta = 10$.

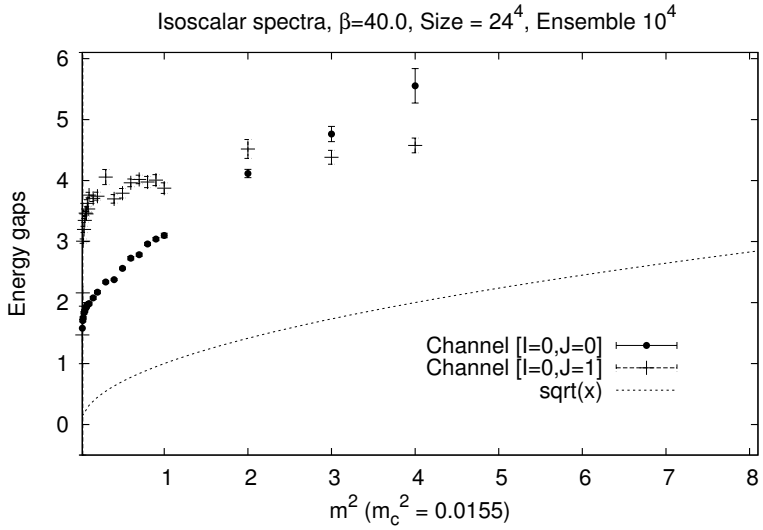

Fig. 9. Mass spectrum ($m \gg m_{\rm c}$) of the isoscalars for $\beta = 40$.

Now, we discuss the region where $m_{\rm c} \leq m < 1$. For large β ($\beta = 3, 10, 40$), two exponentials (see Eq. (15)) are necessary in the region $m^2 \sim m_{\rm c}^2$ in order to fit the time correlators (13). For $\beta = 1.5$, a single exponential fit works well also for values of $m \sim m_{\rm TL}$, where the inflection points show up.

The value of m^2, where the bifurcation occurs, is signaled by sudden and very large errors on Δ_1 and Δ_2. The lower energy gap Δ_1 follows the bare value m, the weight b_1 becomes smaller and smaller by approaching $m_{\rm c}$, while, at the same time, Δ_2 and b_2 increase. The two pictures in Fig. 10 show the bifurcation for $\beta = 3$ in the isovector channel. The pictures in Figs. 11 and 12 show a similar phenomenon for $\beta = 3$ in the isoscalar channels ($J = 0, 1$). Our interpretation is that the lower energy gap is responsible for the long range correlation, signaling the *near* fixed point at $\beta \to \infty$. The larger energy gap is associated to the confining mechanism intervening in the crossing of the TL. A set of figures tries to illustrates these facts. In the isovector channel ($J = 1$), the pattern is very clear. By m approaching $m_{\rm c}$, the lower gap $\sim m$ has a vanishing weight, while the higher gap ($\gg m$) becomes dominant.

A similar phenomenon occurs in the channels $I = 0$, $J = 0$ (see Fig. 11) and $I = 0, J = 1$ (see Fig. 12); however, the onset of bifurcation is for lower m values and the patterns are not as clear as in the isovector case.

We have repeated this analysis for $\beta = 10$ and for $\beta = 40$. The features are very similar to the case $\beta = 3$, thus we shall not provide further pictures to illustrate the bifurcation phenomena for these cases.

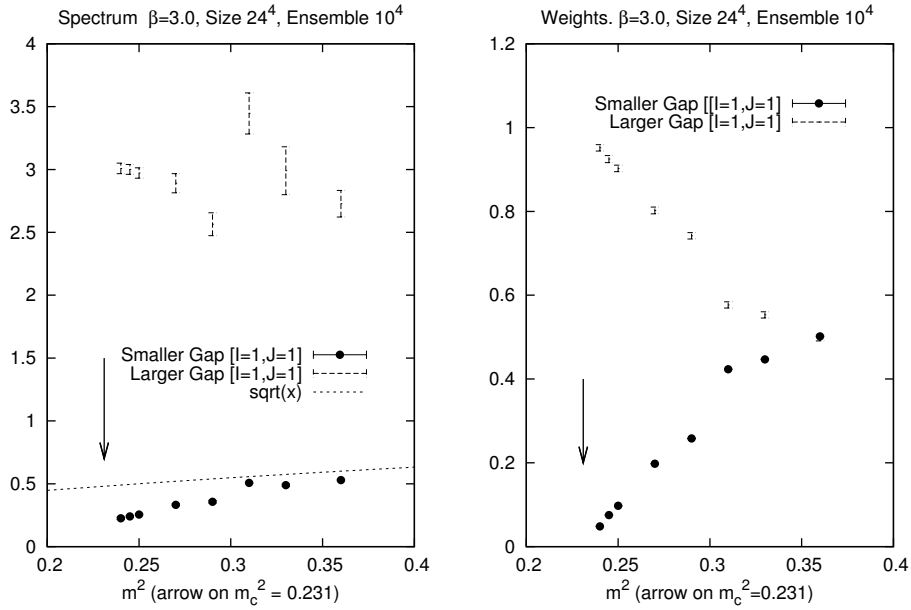

Fig. 10. Mass spectrum and weights ($m_c \leq m$) of the isovector for $\beta = 3$.

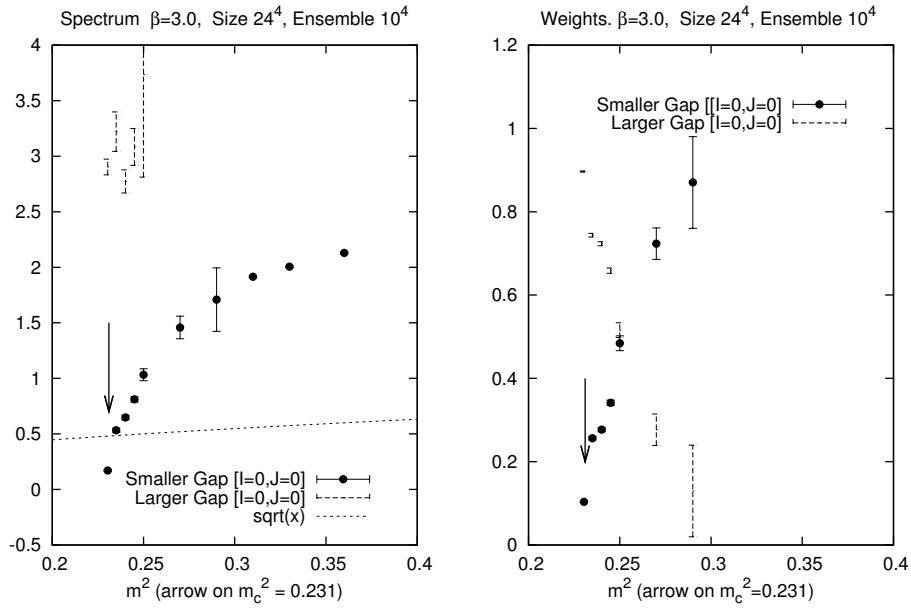

Fig. 11. Mass spectrum and weights ($m_c \leq m$) of the $I = 0$, $J = 0$ for $\beta = 3$.

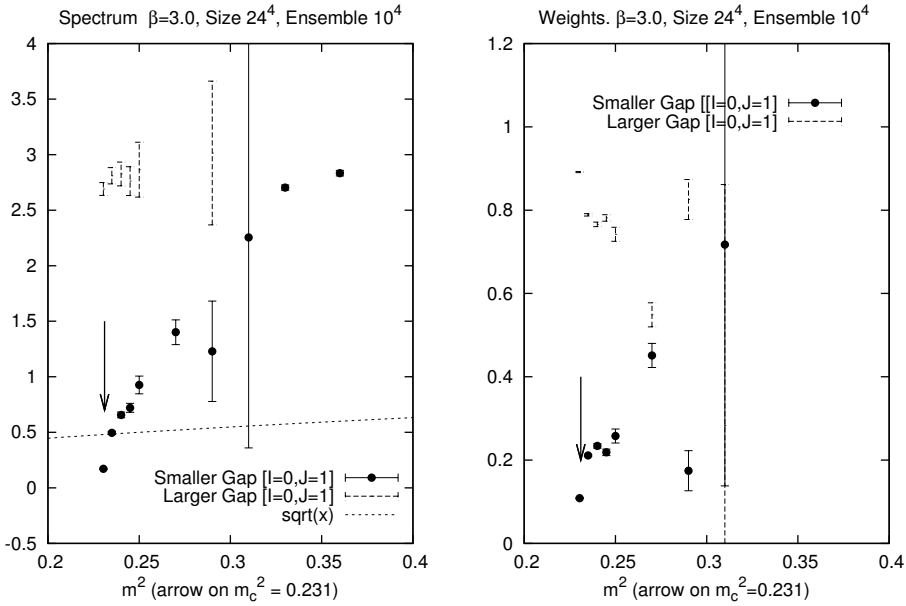

Fig. 12. Mass spectrum and weights ($m_c \leq m$) of the $I = 0$, $J = 1$ for $\beta = 3$.

4.1. Comments on the spectrum

We summarize the comments on the spectrum resulting from the lattice simulations. There is some non-trivial time correlation in the two-point function for the channels with quantum numbers ($I = 1$, $J = 1$), ($I = 0$, $J = 0$) and ($I = 0$, $J = 1$). In the channel $I = 1$ and $J = 0$, we find zero correlation for $t > 0$ in Eq. (13). No fit of the function in Eq. (15) is provided for this channel.

The departure from the bare value m of the energy gap for $m \gg 1$ is common to the values of $\beta = 1.5, 3, 10, 40$.

By approaching $m \sim m_c$, a single exponential fitting of the time correlators is inadequate. A linear combination of two exponentials provides a very good fit. Thus at some value of m (depending on β), the single gap bifurcates: one follows the m line, while the other is much larger. Moreover, the weight of the lower vanishes for $m \to m_c$. This phenomenon is most evident in the channel $I = 1$, $J = 1$. In the other channels, the onset of the bifurcation is faint and at smaller values of m. Our scenario is the following: in approaching the TL, the lower gap provides the large correlation length, while the large gap is the manifestation of the screening/confining mechanism, which becomes dominant for $m \sim m_c$.

For $m \sim m_c$, there are some drastic changes in the energy gaps of the isoscalar channels (for both $J = 0, 1$): one notices a sharp drop, even below the bare value m. This fact sustains the scenario where bound states arise in the isoscalar channels because *(i)* the gap energy becomes lower than the threshold and *(ii)* the vector mesons decouple (very small weight in the two-point functions).

We gratefully acknowledge the warm hospitality of the Center for Theoretical Physics at MIT, Massachusetts, where part of the present work has been done. We profited of many stimulating discussions with the colleagues at the Department of Physics of the University of Pisa.

REFERENCES

[1] R. Ferrari, *Acta Phys. Pol. B* **43**, 1965 (2012) [arXiv:1112.2982 [hep-lat]].

[2] D. Bettinelli, R. Ferrari, *Acta Phys. Pol. B* **44**, 177 (2013) [arXiv:1209.4834 [hep-lat]].

[3] D. Bettinelli, R. Ferrari, A. Quadri, *Phys. Rev.* **D77**, 045021 (2008) [arXiv:0705.2339 [hep-th]].

[4] D. Bettinelli, R. Ferrari, A. Quadri, *Phys. Rev.* **D77**, 105012 (2008) [arXiv:0709.0644 [hep-th]].

[5] R. Ferrari, *J. High Energy Phys.* **0508**, 048 (2005) [arXiv:hep-th/0504023].

[6] R. Ferrari, A. Quadri, *Int. J. Theor. Phys.* **45**, 2497 (2006) [arXiv:hep-th/0506220].

[7] D. Bettinelli, R. Ferrari, A. Quadri, *Int. J. Mod. Phys.* **A23**, 211 (2008) [arXiv:hep-th/0701197].

[8] R. Ferrari, *J. Math. Phys.* **52**, 092303 (2011) [arXiv:1008.2779 [hep-th]].

[9] D. Bettinelli, R. Ferrari, A. Quadri, *Int. J. Mod. Phys.* **A24**, 2639 (2009) [*Erratum ibid.* **A27**, 1292004 (2012)] [arXiv:0807.3882 [hep-ph]].

[10] D. Bettinelli, R. Ferrari, A. Quadri, *Acta Phys. Pol. B* **41**, 597 (2010) [*Erratum ibid.* **43**, 483 (2012)] [arXiv:0809.1994 [hep-th]].

[11] D. Bettinelli, R. Ferrari, A. Quadri, *Phys. Rev.* **D79**, 125028 (2009) [*Erratum ibid.* **D85**, 049903 (2012)] [arXiv:0903.0281 [hep-th]].

[12] R. Ferrari, *J. Math. Phys.* **51**, 032305 (2010) [arXiv:0907.0426 [hep-th]].

[13] R. Ferrari, *Frascati Phys. Ser.* **54**, 268 (2012).

[14] R. Ferrari, *Acta Phys. Pol. B* **43**, 1735 (2012) [arXiv:1106.5537 [hep-ph]].

[15] B.E. Baaquie, G. Bhanot, *Nucl. Phys.* **B382**, 409 (1992).

[16] E.H. Fradkin, S.H. Shenker, *Phys. Rev.* **D19**, 3682 (1979).

[17] J. Jersak, C.B. Lang, T. Neuhaus, G. Vones, *Phys. Rev.* **D32**, 2761 (1985).

[18] H.G. Evertz, J. Jersak, C.B. Lang, T. Neuhaus, *Phys. Lett.* **B171**, 271 (1986).

[19] H.G. Evertz *et al.*, *Phys. Lett.* **B175**, 335 (1986).

[20] I. Campos, *Nucl. Phys.* **B514**, 336 (1998) [arXiv:hep-lat/9706020].

[21] J. Greensite, S. Olejnik, *Phys. Rev.* **D74**, 014502 (2006) [arXiv:hep-lat/0603024].

[22] W. Caudy, J. Greensite, *Phys. Rev.* **D78**, 025018 (2008) [arXiv:0712.0999 [hep-lat]].

[23] C. Bonati, G. Cossu, M. D'Elia, A. Di Giacomo, *Nucl. Phys.* **B828**, 390 (2010) [arXiv:0911.1721 [hep-lat]].

[24] B. Berg *et al.*, "Lattice Higgs. Proceedings", Workshop, Tallahassee, USA, May 16–18, 1988, Singapore: World Scientific, 1988, p. 278.

[25] K.G. Wilson, *Phys. Rev.* **D10**, 2445 (1974).